Journal of Medicinal Chemistry

Article

pubs.acs.org/jmc

Liberation of Copper from Amyloid Plaques: Making a Risk Factor Useful for Alzheimer's Disease Treatment

Jie Geng,[†,‡,§] Meng Li,[†,‡,§] Li Wu,[†,‡] Jinsong Ren,[†] and Xiaogang Qu*[,†]

[†]Laboratory of Chemical Biology, Division of Biological Inorganic Chemistry, State Key Laboratory of Rare Earth Resource Utilization, Changchun Institute of Applied Chemistry, Changchun, Jilin 130022, China

[‡]Graduate School of the Chinese Academy of Sciences, Chinese Academy of Sciences, Beijing 100039, P. R. China

Supporting Information

ABSTRACT: Alzheimer's disease (AD) is a complex multifactorial syndrome. Metal chelator and Aβ inhibitor are showing promise against AD. In this report, three small hybrid compounds (**1**, **2**, and **3**) have been designed and synthesized utilizing salicylaldehyde (SA) based Schiff bases as the chelators and benzothiazole (BT) as the recognition moiety for AD treatment. These conjugates can capture Cu^{2+} from Aβ and become dimers upon Cu^{2+} coordination and show high efficiency for both Cu^{2+} elimination and Aβ assembly inhibition. Besides, the complexes have superoxide dismutase (SOD) activity and significant antioxidant capacity and are capable of decreasing intracellular reactive oxygen species (ROS) and increasing cell viability. All these results indicate that the multifunctional metal complexes which have Aβ specific recognition moiety and metal ion chelating elements show the potential for AD treatment. Therefore, our work will provide new insights into exploration of more potent amyloid inhibitors.

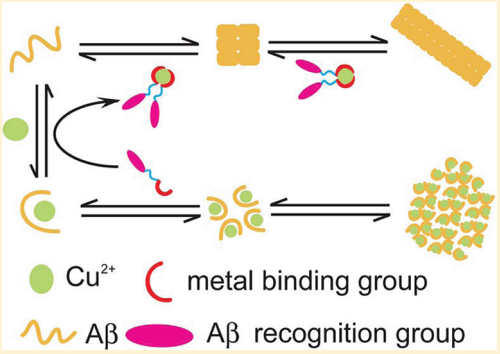

INTRODUCTION

Alzheimer's disease (AD) is the most common form of dementia, which affects more than 15 million people worldwide.[1] This figure is projected to double every 20 years as a result of an increasing life span. AD is characterized by cerebral extracellular amyloid plaques and intracellular neurofibrillary tangles.[2] The amyloid β peptide (Aβ) with 39−42 residues is the major component of amyloid plaques found in brains of AD patients. Although the molecular mechanisms of AD pathogenesis have not been clearly understood due to its complexity, recent advances have demonstrated that polymerization of Aβ into amyloid fibrils is a critical step in the pathogenesis.[2] The origin of insoluble extracellular neurotoxic deposits is still not clear, and multiple factors such as pH, temperature, protein concentration, and ionic strength have been reported to trigger their formation.[3] Therefore, the inhibition of Aβ assembly has been considered as the primary therapeutic strategy for the neurodegenerative diseases.

Metal ions are involved in the assembly and neurotoxicity of Aβ species.[4] Copper, concentrated in amyloid plaques (≈0.4 mM), is involved in the pathogenesis of AD.[5] Cu^{2+} is able to accelerate the formation of Aβ aggregates and influence their conformational transformation.[6] In addition, the Aβ-bound Cu^{2+} can contribute to the formation of neurotoxic reactive oxygen species (ROS).[7] Therefore, metal-ion chelation therapy as a treatment for AD has been explored to prevent Aβ deposition and ROS production.[8]

Peptide or peptide mimetics[9] and small organic molecules with aromatic groups[10] are now the two main classes of Aβ inhibitors. The hydrophobic core KLVFFA, positioned at the β1 region in the structural model of Aβ1−40 fibrils, is crucial for the self-assembly of Aβ into fibrils. Short peptides containing the core sequence have been used as "binding element" to design the inhibitors of fibrillization. A number of low-molecular-mass Aβ aggregation inhibitors have also been identified by screening of compound libraries as well as rational design strategies. The resulting inhibitors include such chemically diverse compounds as curcumin, (−)-epigallocatechingallate (EGCG), and rifampicin. However, a majority of the above inhibitors show only moderate inhibition efficiency attributed to their poor ability to interact over the large interface of interaction of Aβ peptides during the aggregation process or to interact simultaneously with the multiple binding surfaces.[11] Therefore, there is ever-increasing demand for designing novel more potent AD inhibitors.

Evidences support the hypothesis that ligands exhibiting greater affinity for the β-amyloid peptide are more effective at preventing amyloid formation and inhibiting amyloid neurotoxicity.[12] The use of multiple simultaneous interactions to enhance target binding affinity and specificity is an important concept and versatile in biology. Therefore, development of new multimeric molecules used for AD therapy has received much attention in recent years.[13] These multimeric molecules

Special Issue: Alzheimer's Disease

Received: March 19, 2012
Published: June 4, 2012

dx.doi.org/10.1021/jm3003813 | J. Med. Chem. 2012, 55, 9146−9155

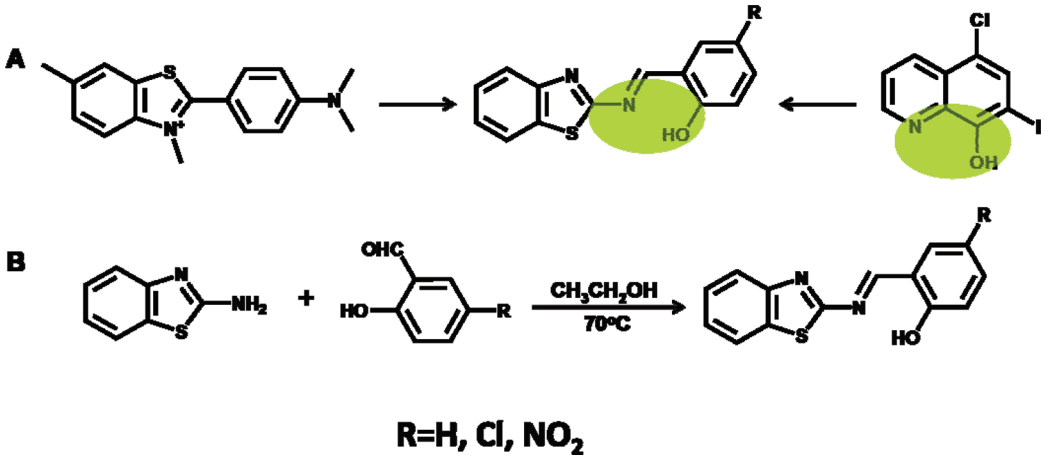

Figure 1. (A) Combination of the main features of ThT and CQ provides new ligands with potential intercalating and chelating properties. (B) Synthesis of compounds **1**–**3**. Compound **1**, R = H; compound **2**, R = Cl; compound **3**, R = NO_2.

show stronger ability to block fibril formation than the corresponding monomers. Molecular self-assembly, which combines the facile multimerization observed in the family of antibodies, and the improved binding affinity and specificity of synthetic organic molecules represent an intriguing hybrid approach to targeting amyloid.[13]

Metal complexation has been used as scaffold to design three- or four-helix bundles.[14] Considering the high concentration of Cu^{2+} in amyloid plaques, combining metal complexation and ligand interaction may offer a novel method to construct multivalent Aβ inhibitors. Benzothiazole is known to possess binding affinity for β-amyloid plaques when appropriately derivatized and has been used as essential part of some imaging agents for β-amyloid plaques.[15] Thus, we designed and synthesized three small hybrid compounds, (*E*)-2-((benzo[*d*]-thiazol-2-ylimino)methyl)phenol **1**, (*E*)-2-((benzo[*d*]thiazol-2-ylimino)methyl)-4-chlorophenol **2**, and (*E*)-2-((benzo[*d*]-thiazol-2-ylimino)methyl)-4-nitrophenol **3** (Figure 1) utilizing salicylaldehyde based Schiff bases as the chelators and benzothiazole as the recognition moiety. These conjugates are designed to become dimers due to Cu^{2+} coordination, holding great promise for Cu^{2+} elimination and Aβ assembly inhibition abilities.

RESULTS AND DISCUSSION

Prediction of BBB Penetration of compound 1, 2, and 3. A major impediment to the development of effective anti-Aβ compounds for AD therapy is that essentially 100% of large-molecule drugs and >98% of small-molecule drugs fail to cross the blood–brain barrier (BBB).[16] Filters to ensure that the resultant molecules fulfill drug-like criteria that are most commonly defined using Lipinski's rules:[17] molecular weight (MW) less than 500, the calculated logarithm of the octanol–water partition coefficient (clogP) less than 5, the number of hydrogen bond donor atoms (HBD) less than 5, and the number of hydrogen-bond acceptor atoms (HBA) less than 10. Filter for prediction of BBB penetration involves calculation of log BB by means of the equation shown in the footnote of Table 1. This equation has shown good predictive ability and comprises two simple variables that can be rapidly computed for any structure: clogP and the topological polar surface area (TPSA). The multifunctional small molecules were prepared via Schiff base condensation between benzothiazole and salicylaldehyde or its derivates (Figure 1). By changing the R group on the salicylaldehyde, the aqueous solubility, lipophilicity, and BBB permeability can be modified. Defined by the restrictive terms of Lipinski's rules and calculated log BB for potential applications in brains, compounds **1**–**3** fulfil drug-like criteria and possible brain penetration (Table 1).

Table 1. Physical Properties of XSABT Ligands Used in Our Studies

calculation[a]	1	2	3	rules
MW	254.05	288.75	299.30	≤450
clogP	1.80	2.52	1.55	≤5.0
HBA	3	3	6	≤10
HBD	1	1	1	≤5
log BB	−0.26	−0.15	−0.97	≥-1.0

[a]MW: molecular weight. clogP: calculated logarithm of the octanol–water partition coefficient. HBA: hydrogen-bond acceptor atoms. HBD: hydrogen-bond donor atoms. log BB = −0.0148 × PSA + 0.152 × clogP + 0.130.

Chelating Properties of Compounds toward Cu^{2+}. All of the three compounds were studied by UV–vis spectroscopy to determine their ability to act as Cu^{2+} chelators.[18] To this end, spectrophotometric titrations were used for the Cu^{2+} binding. As an example, a series of UV–vis spectra of compound **1** titrated by Cu^{2+} were shown in Figure 2, while the spectra of compound **2** and **3** were given in Figure S1 in Supporting Information. In the absence of Cu^{2+}, the UV–vis spectrum of compound **1** showed absorption maximum at 375 nm and a shoulder at 330 nm. When Cu^{2+} was added, a new band at 460 nm appeared which was associated with the copper complex. Therefore, the binding stoichiometry of compound **1** with $CuCl_2$ was determined by following the absorption changes at 460 nm. The presence of an isosbestic point revealed the formation of a unique Cu^{2+}–**1** complex (Figure 2), and titration analysis was consistent with a 1:2 Cu^{2+}/ligand molar ratio (Figure 2 inset). We have also made an attempt to estimate the binding affinity of compound **1** to Cu^{2+} and the log K_b value for the 2:1 complex was calculated to be 13. For Cu^{2+}, the binding affinity follows the order **1** > **2** > **3**, which was consistent with the general rule for a series of similar ligands that the binding constants increased with increasing ligand basicity.

To explore the metal binding properties of compounds **1**–**3** with other biologically relevant metal ions, the optical

dx.doi.org/10.1021/jm3003813 | *J. Med. Chem.* 2012, 55, 9146–9155

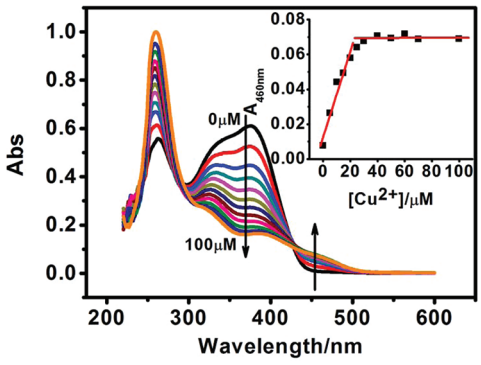

Figure 2. UV−vis titration of compound **1** with Cu^{2+} in 50% (v/v) DMSO/buffer (10 mM HEPES, 150 mM NaCl, pH 6.6) at room temperature. The concentration of Cu^{2+} was varied from 0 to 100 μM. Inset: change in absorbance at 460 nm with increased concentration of Cu^{2+} derived from the UV−vis titration, a breakpoint was observed at 0.5:1 ratio. The concentration of compound **1** was 50 μM.

responses of compounds **1**−**3** in the presence of other metal ions (Mg^{2+}, Ca^{2+}, Al^{3+}, Fe^{3+}, Co^{2+}, or Ni^{2+}) were examined[19] as depicted in Figure S2A,C,E in Supporting Information. Taking compound **1** for example, less optical changes were observed upon incubation of ligands with these metal ions. Then the selectivity of compound **1** for Cu^{2+} in the presence of other divalent metal ions was investigated by UV−vis (Figure S2B in Supporting Information). The optical intensity at 460 nm (absorption band for Cu^{2+}-treated compound **1**) was monitored when the appropriate metal ions (25 μM) were added to a 50 μM solution of compound **1** followed by the subsequent treatment with 25 μM Cu^{2+}. As shown in Figure S2B in Supporting Information, binding of compound **1** (50 μM) to Cu^{2+} (25 μM) was observed in the presence of other metal ions (25 μM), which indicated that compound **1** was selective to Cu^{2+}. Similar results were observed for compound **2** but not **3**, which showed relatively poor Cu^{2+} selectivity.

Copper is concentrated in amyloid plaques and directly coordinates Aβ at the histidine side chains in its amino terminus.[4] We next investigated Cu^{2+} transfer from Aβ to compounds **1**−**3** by UV−vis spectra. Upon adding compounds **1**−**3** to Cu^{2+}−Aβ, the UV−vis spectrum changed steadily toward the typical spectrum of Cu^{2+}−**1**, **2**, and **3** (Figure S3 in Supporting Information). The competitive binding of compounds **1**−**3** for Cu^{2+} suggested that the chelators would sequester Cu^{2+} from Aβ and therefore inhibited Cu^{2+} induced Aβ aggregation.

Inhibition of Cu^{2+} Induced Aβ Aggregation. Cu^{2+} is known to cause Aβ aggregation in solution, and the interaction of Aβ peptide with Cu^{2+} is known to be pH dependent. It has been reported that Cu^{2+}-induced Aβ aggregation is more significant at pH 6.6 than at pH 7.4.[6a] To investigate the influence of ligands on Cu^{2+}-induced Aβ aggregation, we performed two individual studies in a weak acidic buffered aqueous solution: inhibition (the prevention of forming metal-induced Aβ aggregates) and disaggregation (the transformation of metal−Aβ aggregates by chelators). The effect of ligands on metal-induced Aβ1−40 aggregation was assessed, and clioquinol (CQ) was used as a positive control because CQ is known to attenuate metal ion−Aβ aggregation.[8] The degree of Aβ aggregation was probed mainly by light scattering, which exhibited the change in solution turbidity as a result of precipitate formation,[20] and atomic force microscopy (AFM), which showed the morphology of Aβ aggregates.[21]

Synthetic human Aβ1−40 was dissolved in a buffered aqueous solution (10 mM HEPES, pH 6.6, 150 mM NaCl, 2-[4-(2-hydroxyethyl)-1-piperazinyl] ethanesulfonic acid (HEPES)) to which Cu^{2+} was added. Addition of metal ion caused significant Aβ aggregation, which was monitored by recording the light scattering on a fluorescence spectrophotometry (Figure 3). Higher light scattering at 320 nm (LS_{320}) of

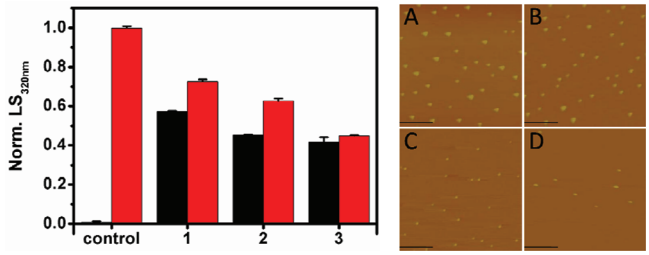

Figure 3. Inhibition and disaggregation of Cu^{2+}-induced Aβ aggregates by chelators. Left: Effect of chelators on the Cu^{2+}-induced Aβ aggregation was evaluated by the change of LS at 320 nm. Black, inhibition experiments; red, disaggregation experiments. Right: The morphology of Aβ aggregates after 24 h incubation without (A) or with (B) compound **1**, (C) **2**, or (D) **3** was analyzed by AFM (disaggregation experiments). Scale bars: 500 nm. Inhibition experiments: compounds **1**−**3** was added before incubation of Aβ−Cu^{2+}. Disaggregation experiments: **1**−**3** was added after 24 h incubation of Aβ−Cu^{2+}. [Aβ] = 10 μM; [Cu^{2+}] = 10 μM; [**1**], [**2**], or [**3**] = 20 μM. Buffer: 10 mM HEPES, 150 mM NaCl, pH 6.6.

the resultant solution indicated more aggregates existing. The presence of 2 equiv of compounds **1**−**3** inhibited Cu^{2+}-induced aggregation significantly. Metal-associated aggregation could also be attenuated upon subsequent addition of ligand. Addition of metal-binding ligands to Aβ−Cu^{2+} aggregates reduced the scattering by varying extents (Figure 3). Morphological analysis of Aβ aggregates on the surface of mica formed by interaction between Aβ40 and Cu^{2+} with or without chelators was achieved by AFM. Sample without a chelator showed a lot of Aβ40 deposits (Figure 3), while in the samples with compounds **1**−**3**, the large plaques of amorphous Aβ40 aggregates became smaller and fewer (Figure 3B−D).

The Cu^{2+} trials showed that all the chelators significantly reduced the amount of aggregated Aβ in the solution. Interestingly, the relative disaggregation activities of the three ligands were higher than that of CQ for the Cu^{2+} trials, despite the large difference in metal binding affinity (Figure S4 in Supporting Information). Aβ targeted metal chelator is known to result in better modulation of Aβ aggregation.[22] We speculated that the increased disaggregation activity of compounds **1**−**3** could be due to Aβ intercalating ability of these benzothiazole compounds.

Inhibition of Aβ Self-Assembly. Molecular self-assembly, which is the spontaneous association of molecules under equilibrium conditions into stable, structurally well-defined aggregates that are joined by noncovalent bonds, is ubiquitous in biological systems and underlies the formation of a wide variety of complex biological structures. An interesting goal of molecular assembly is to obtain biomolecules to display multivalent interactions, which are characterized by simultaneous binding of multiple ligands on one biological entity to multiple receptors on another with high avidity.[23] Various

dx.doi.org/10.1021/jm3003813 | J. Med. Chem. 2012, 55, 9146−9155

approaches have been developed to engineer multivalency by linking multiple ligands together.[24] Considering the general Cu^{2+} content in the AD brain is at least 1 order of magnitude higher than that in the blood, we suggest that the compounds **1**−**3** can selectively assemble to dimer in the brain (Figure S5 in Supporting Information), which is able to inhibit Aβ self-assembly effectively.

We first compared the Aβ binding affinity of compounds **1**−**3** and their copper complexes. Taking advantage of the Aβ tyrosine fluorescence quenching effect of the compounds, the apparent binding constants[6d] yielded by nonlinear least-squares fitting (Figure S6 in Supporting Information) were shown in Table 2. All the copper complexes exhibited stronger binding affinity than their ligands with an enhancement of one order due to the multivalent effect, which meant that these complexes might have stronger Aβ aggregation inhibition ability.[12]

Table 2. K_b (Binding Constant) of Chelators or Their Copper Complexes to Aβ

	1	2	3
ligand	1.0×10^5 M^{-1}	3.2×10^5 M^{-1}	8.9×10^5 M^{-1}
complex	1.9×10^6 M^{-1}	1.8×10^6 M^{-1}	7.3×10^6 M^{-1}

To directly compare the effects of compounds **1**−**3** and their copper complexes **4**−**6** on Aβ aggregation, Aβ1−40 was incubated for 7 days in the presence of chelators or their copper complexes in different ratios. The ratios were expressed per mole of ligand. Thioflavin T (ThT) analysis showed that **4**−**6** inhibited Aβ1−40 aggregation in a concentration dependent manner; the strongest inhibition occurred at the highest concentration used (Figure 4). Taking **6** for example, a 1:2 ratio of Aβ/**3** (in **6**) inhibited the relative change of ThT fluorescence by more than 75%, whereas the same ratio of **3** inhibited ThT by only 35% (Figure S8 in Supporting Information). **6** was a stronger potent inhibitor of Aβ aggregation than **3**, which was consistent with our expectation. As to compound **1** and **2**, neither of them showed any inhibition (Figure S7 in Supporting Information), while their Cu^{2+} complexes exhibited significant ability to prevent Aβ fibrillization (Figure 4).

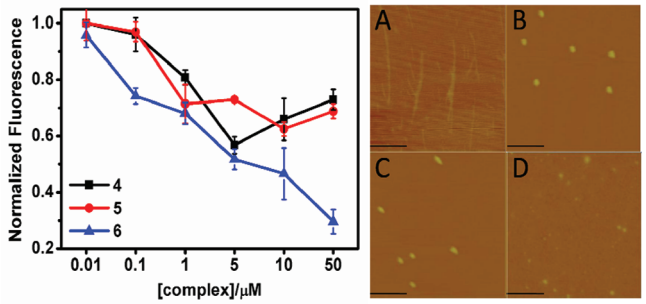

Figure 4. Inhibition of Aβ self-assembly by metal complex. Left: Concentration-dependent inhibition of Aβ fibrillogenesis assessed by ThT assay. Right: The morphology of Aβ aggregates was analyzed by AFM images in the absence (A) or presence of **4** (B), **5** (C), or **6** (D). Aβ was fixed at 50 μM and was mixed with **4**−**6**. Aliquots were kept at 37 °C for 7 days after being mixed. All the reactions were conducted without agitation. Buffer: 10 mM HEPES, 150 mM NaCl, pH 7.3. Scale bars: 500 nm.

AFM was used to determine the morphology of the Aβ40 assembly when maximal ThT binding was observed. Classical amyloid fibrils were observed in samples of untreated Aβ40 (Figure 4A).[21] The Aβ40 fibrils were nonbranched, helical filaments with diameters of ∼10 nm and lengths of up to several micrometers. The addition of compounds **1**−**3** (100 μM concentration) could hardly or only slightly alter the assembly of Aβ40 (date not shown). In contrast to the results with compounds **1**−**3**, stronger inhibition of fibril assembly was observed in **4**-, **5**-, and **6**-treated samples at the same concentrations. In addition, numerous small, relatively amorphous aggregates were observed (Figure 4B−D).

We next performed a variety of experiments in order to determine whether these metal complexes could dissociate the existing fibrils of Aβ. The addition of complexes after the completion of the fibrillation reaction, as monitored by ThT, led to a rapid, concentration dependent decrease in fluorescence signal that was consistent with loss of fibrils, whereas in controls with no complexes, the ThT signal remained essentially constant (Figure 5). AFM experiments further supported that the metal complexes **4**−**6** could remarkably decrease fibril numbers (Figure 5) while increasing the amorphous aggregates.

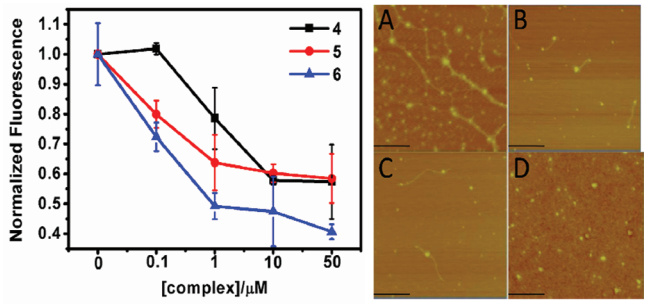

Figure 5. Disassembly of Aβ fibrils by **4**−**6**. Left: Concentration-dependent disassembly of Aβ fibrillogenesis assessed by ThT assay. Right: The morphology of Aβ was analyzed by AFM in the absence (A) or presence of **4** (B), **5** (C), or **6** (D). Aβ was fixed at 50 μM and fibrillar Aβ40 was mixed with **4**−**6**. Aliquots were kept at 37 °C for 24 h after being mixed. All the reactions were conducted without agitation. Buffer: 10 mM HEPES, 150 mM NaCl, pH 7.3. Scale bars: 500 nm.

The 1:2 copper complexes of **1**−**3**, having a high binding constant, are expected to be stable in biological solutions, without undergoing hydrolysis. They are desired to be more stable than the ones formed by mixing the two reagents. Upon Aβ binding, the metal-to-ligand charge-transfer (MLCT) bands of the metal complexes did not change (Figure S8 in Supporting Information), indicating that Aβ binding did not destroy the complex structure.

The influence of copper ions on aggregation of Aβ has been intensively studied over the past decade. Nevertheless, many important aspects like the effect of metal ions on aggregation kinetics and the effect of chelators on metal-induced aggregation of Aβ are still elusive. In early studies, metal ions have been reported to enhance the rate of Aβ fibrillization and metal chelators acted in an opposite direction by reversing the aggregation.[6,7] Later on, evidence demonstrate that metal-induced Aβ aggregates are predominantly nonfibrillar.[25] Recent results show that the aggregated state of Aβ peptide in vitro depended on the concentration of Cu^{2+}. Image study indicates

dx.doi.org/10.1021/jm3003813 | J. Med. Chem. 2012, 55, 9146−9155

that at low concentrations of Cu^{2+}, the aggregates are mature fibrils, whereas at high Cu^{2+} concentrations, granular aggregates are formed.[26] Medium- and high-affinity metal chelators including metallothioneins can initiate fast Aβ42 fibrillization.[27] Consequently, the outcome of metal-chelation therapy might vary between two opposite scenarios: removal of metal ions especially of Cu^{2+} and reduction of their toxicity; solubilization of metal induced Aβ aggregates and promotion of Aβ fibrillization and amyloid formation under certain conditions, which threw the chelator therapy into a dilemma. Thus, alternative mechanisms should be applied to stop amyloidogenesis and reduce amyloid load of AD patients. As demonstrated above, compounds **1**−**3** can remove Cu^{2+} from Aβ and reduce their toxicity, and the formed metal complexes **4**−**6**, on the other hand, can inhibit Aβ fibrillization and disassemble formed Aβ fibrils (Figure 6). Therefore, our strategy described here may shed light on how to design more potent amyloid inhibitors.

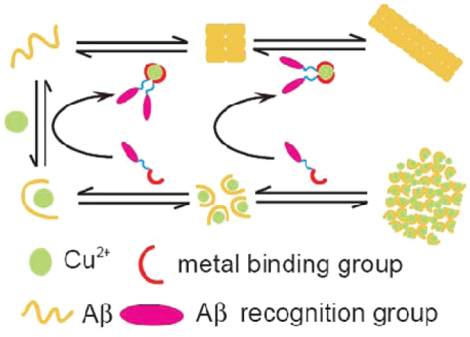

Figure 6. Schematic representation of the possible modes of multifunctional effects of our chelators in the process of Aβ aggregation. Aβ exists in equilibrium between monomers, oligomers, and amyloid fibrils, while Cu^{2+} binds to Aβ monomer and prevents amyloidogenesis by inducing the formation of nonfibrillar aggregates. Our chelators **1**−**3** can disassembly Cu^{2+} induced Aβ aggregates through sequestration of Cu^{2+} from Aβ and the formed multivalent complexes have strong inhibition and dissolution ability in Aβ fibrillization.

Inhibition of H_2O_2 Production. The formation of ROS by Cu−Aβ has been suggested as another proposed mechanism of AD pathogenesis.[7,28] This could cause an increase in oxidative stress, which triggers damage of cellular components such as DNA, lipids, and proteins.[29] Under reducing conditions, the Aβ−Cu complex reacts with O_2 to generate H_2O_2. The effects of the chelators on the generation of H_2O_2 by compounds **1**−**3** were examined in cell-free solutions by a widely used horseradish peroxidase (HRP)/luminol chemiluminescence assay. Samples containing Cu^{2+}, Aβ, and compounds **1**−**3** showed less H_2O_2 at different levels (Figure 7), indicating that all compounds **1**−**3** could reduce H_2O_2 produced by Cu−Aβ.

SOD (Superoxide Dismutase) Activity of Metal Complexes. Partial deficiency of SOD-2, which plays an important role in the clearance of ROS, has been shown to accelerate plaque deposition[30] and increase tau phosphorylation in AD mice models.[31] SOD-2 deficiency has also been shown to accelerate the onset of a number of behavioral deficits in hAPP mice.[32] Overexpression of SOD-2 reduces hippocampal superoxide and prevents memory deficits in a mouse model of Alzheimer's disease.[33] Overexpression of Mn-SOD or addition of MnTE-2-PyP^{5+} (SOD mimic) can protect against

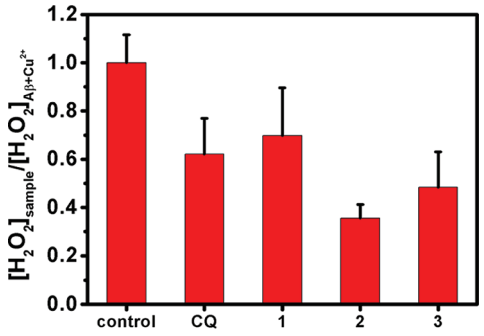

Figure 7. Production of H_2O_2 from reactions of Aβ, Cu^{2+}, and compound upon addition of ascorbate, as determined by a HRP/luminol assay. Control: Aβ + Cu^{2+}. [Aβ] = 10 μM, [Cu^{2+}] = 20 μM, [chelator] = 40 μM, [ascorbate] = 50 μM, [luminol] = 10 μM, [HRP] = 3 U/mL.

β-amyloid-induced neuronal death and improve mitochondrial respiratory function.[34] Considering the fact that the active centers of superoxide dismutase (SOD) are metal complexes, we speculate that although the chelator is inert, when the chelator captures Cu from Aβ−Cu complex, the formed chelator−Cu complex may form an active artificial enzyme center and show SOD activity.

The SOD activity of the chelator−Cu complex was quantified using a modified NBT assay system.[35] Superoxide anion generation by the system was detected using spectroscopy by following reduction of nitro blue tetrazelium (NBT) to blue formazane (MF^+) at 560 nm. To determine the activity of the enzyme mimics, we measured the IC_{50} values of the reactions, a generally used indicator for comparing the activity of enzyme and enzyme mimics. The results indicated that all copper complexes had SOD activity as expected while their corresponding ligands showed little SOD activity (Figure S9A in Supporting Information). IC_{50} values of the prepared complexes were 1.31, 1.06, and 0.19 μM, respectively (Figure 8), and **6** was the most potent SOD mimic where the presence of aromatic rings in the vicinity of metal center led to the enhanced SOD activity. The results also indicated that copper atom was essential for SOD activity and incorporation of copper into the structure of antioxidant could tremendously increase the mimic SOD activity. Besides, we adopted SOD enzyme as reference to compare with these complexes (Figure

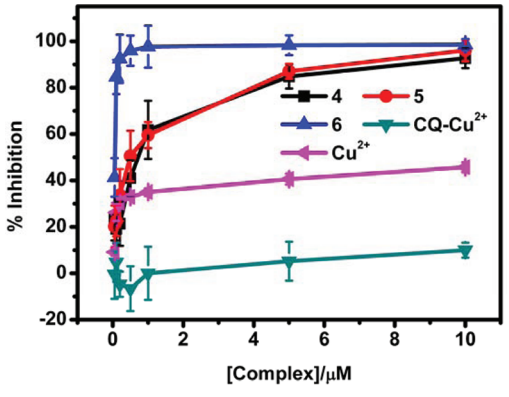

Figure 8. Percentage inhibition of NBT oxidation by superoxide radicals generated in riboflavin−NBT−light system in vitro assessed by NBT^+ absorption at 560 nm with CQ−Cu^{2+}, **4**, **5**, or **6** ([ligand]:[Cu^{2+}] = 2:1).

dx.doi.org/10.1021/jm3003813 | J. Med. Chem. 2012, 55, 9146−9155

S9B in Supporting Information). The amounts of the complexes equivalent to 1U of enzyme activity were 9, 7.5, and 0.2 μM, respectively. Therefore, the prepared complexes of low molecular weight and simple structures could be SOD mimics as proposed.

Intracellular Determination of ROS. There is abundant evidence of peroxidative attack in AD brain,[28] which may originate from Aβ–Cu electrochemistry.[36] Exposure of the cells to 5 μM Aβ–Cu caused 194% increase in content of ROS relative to Aβ–Cu-untreated control cells (Figure 9). Pretreatment of the cells with compounds **1**–**3** at concentrations of 10 μM diminished the levels of ROS by 25%, 27%, and 41%, respectively, compared to the cells exposed only to Aβ–Cu. The intracellular level of ROS did not vary among the cells treated solely with Aβ (5 μM). On the basis of these data, the formed Cu complex could be a free-radical scavenger.

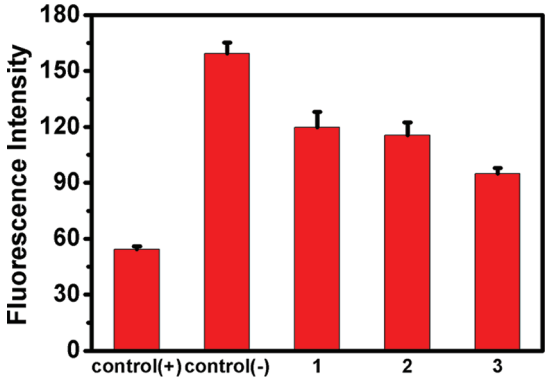

Figure 9. Cells were treated with aged Aβ40–Cu^{2+} at the concentration of 5 μM in the absence or presence of ligands (10 μM), and 12 h later ROS generation inside the cells was measured using DCF fluorescence. Samples (from left to right) are: control, Aβ–Cu(II), Aβ–Cu(II) + **1**, Aβ–Cu(II) + **2**, Aβ–Cu(II) + **3**. Data represents mean ± SEM of at least three different experiments.

Radical scavengers and metal chelators have been scrutinized in clinical studies of AD and positive results have been gained in the past few years which have the ability to attenuate the broad spectrum of oxidative stress associated neuropathology, as well as APP translation, Aβ generation, and amyloid plaques and NFT formation. It was proposed that if one compound held radical-scavenging and metal–protein-attenuating properties simultaneously, it might be more potent than that with single property, inspired by the preliminary successes of radical scavengers and metal–protein-attenuating compound (MPAC).[37]

Cell Viability Assay. The ability of compounds **1**–**3** to inhibit Aβ assembly suggested that it might be useful in blocking Aβ-mediated cellular toxicity. To address this question, we used PC12 cells to perform MTT assays to probe cellular metabolism.[38] All assays were carried out in the same manner, and the data were normalized using the results from the cells not treated with Aβ–Cu^{2+} as a positive control. Treatment of the cells with 5 μM Aβ–Cu^{2+} for 2 days reduced cell viability to 58%. In the presence of compounds **1**–**3**, the survival of the cells increased to about 90% (Figure 10). The survival rate was even higher than that of CQ (Figure 10). As depicted in Figure S10 in Supporting Information, the multifunctional compounds **1**–**3** themselves exhibited less toxicity than the clinically available compound CQ. These results showed that compounds **1**–**3** were not only effective as in vitro Aβ inhibitors but also could decrease Aβ-mediated cellular toxicity.

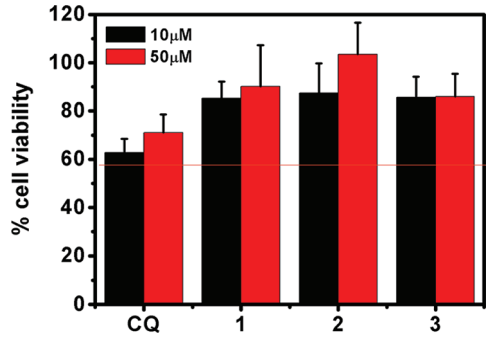

Figure 10. Protection effects of ligands on Aβ40–Cu^{2+}-induced cytotoxicity of PC 12 cells. Cell viability was determined using MTT method and data points shown are the mean values ± SEM from three independent experiments.

CONCLUSIONS

Alzheimer's disease (AD) is a complex multifactorial syndrome unlikely to arise from a single causal factor. Different number of related biological alterations may contribute to AD pathogenesis.[39] None of the presently marketed drugs, although valuable in improving cognitive, behavioral, and functional impairments, can alter AD progression.[40] Design of multifunctional molecules may provide new insights into developing more potent amyloid inhibitors. Here, we have shown that the benzothiazole-containing compounds **1**–**3** can bind Cu^{2+} and decrease Aβ-mediated cellular toxicity. More importantly, these chelators can change copper from risk factor into useful species. Compounds **1**–**3** can bind Cu^{2+} and assemble into metal complexes, which are not only able to inhibit Aβ self-aggregation but also to dissolve the formed fibrils due to multivalent effect. In addition, the formed metal complexes have significant SOD activity and therefore can act as a free-radical scavenger. Our results strongly support the designed mechanism of action that the compounds can compete effectively for copper with the metal binding sites on Aβ peptide, inhibit Aβ self-assembly, and function as antioxidants and reduce Aβ cellular toxicity. This may open an avenue for exploration of more potent amyloid inhibitors.

EXPERIMENTAL SECTION

Materials. All of the solvents were reagent grade and used without further purification unless otherwise specified. The commercial compounds $CuCl_2{\cdot}2H_2O$, salicylaldehyde, 5-chlorosalicylaldehyde, 5-nitrosalicylaldehyde, 2-aminobenzothiazole, clioquinol, and thioflavin T were purchased from Sigma-Aldrich. 1,1,1,3,3,3-Hexafluoro-2-propanol (HFIP) and 4,4′-methylenedianiline were obtained from Acros organics. Milli-Q water was used to prepare all of the buffer solutions.

(*E*)-2-((Benzo[*d*]thiazol-2-ylimino)methyl)phenol (1). **1** was prepared by Schiff base condensation of salicylaldehyde (5 mmol) with 2-aminobenzothiazole (5 mmol) in ethanol (40 mL), at reflux for 8 h. After cooling, the Schiff base precipitated from the reaction mixture as a pure yellow powder, washed with ethanol three times, and then dried in vacuum (purity >95%). ^{1}H NMR (400 MHz, $CDCl_3$, 25 °C): δ = 12.23 (H, s), 9.28 (H, s), 7.99–7.97 (H, d), 7.86–7.84 (H, d), 7.53–7.46 (3H, m), 7.41–7.39 (H, t), 7.08–7.05 (H, d), 7.02–7.00 (H, t). MALDI-TOF-MS ($CHCl_3$): m/z 255.1, $[M + H]^+$. Elemental Anal., Calcd %: C, 66.12; H, 3.96; N, 11.02. Found %: C, 65.96; H, 3.92; N, 10.69.

dx.doi.org/10.1021/jm3003813 | J. Med. Chem. 2012, 55, 9146–9155

(*E*)-2-((Benzo[*d*]thiazol-2-ylimino)methyl)-4-chlorophenol (2). **2** was prepared by Schiff base condensation of 5-chlorosalicylaldehyde (5 mmol) with 2-aminobenzothiazole (5 mmol) in ethanol (40 mL) at reflux for 8 h. After cooling, the Schiff base precipitated from the reaction mixture as a pure yellow powder, washed with ethanol three times, and then dried in vacuum (purity >95%). ^{1}H NMR (400 MHz, $CDCl_3$, 25 °C): δ = 12.21 (H, s), 9.22 (H, s), 8.00−7.98 (H, d), 7.87−7.85 (H, d), 7.53−7.48 (2H, m), 7.42−7.38 (2H, m), 7.03−7.01 (H, d). MALDI-TOF-MS ($CHCl_3$): m/z 289.0, $[M + H]^+$. Elemental Anal., Calcd %: C, 58.23; H, 3.14; N, 9.70. Found %: C, 58.47; H, 3.41, N, 9.64.

(*E*)-2-((Benzo[*d*]thiazol-2-ylimino)methyl)-4-nitrophenol (3). **3** was prepared by Schiff base condensation of 5-nitrosalicylaldehyde (5 mmol) with 2-aminobenzothiazole (5 mmol) in ethanol (40 mL), at reflux for 8 h. After cooling, the Schiff base precipitated from the reaction mixture as a pure yellow powder, washed with ethanol three times, and then dried in vacuum (purity >95%). ^{1}H NMR (400 MHz, $CDCl_3$, 25 °C): δ = 13.10 (H, s), 9.40 (H, s), 8.53−8.52 (H, d), 8.37−8.34 (H, d), 8.04−8.01 (H, d), 7.91−7.89 (H, d), 7.57−7.53 (H, t), 7.46−7.42 (H, t), 7.19−7.16 (H, d). MALDI-TOF-MS ($CHCl_3$): m/z 300.0, $[M + H]^+$. Elemental Anal., Calcd %: C, 56.18; H, 3.03; N, 14.04. Found %: C, 55.93; H, 2.99, N, 13.96.

(*E*)-2-((Benzo[*d*]thiazol-2-ylimino)methyl)phenol−$CuCl_2$ (4). $CuCl_2{\cdot}2H_2O$ (0.017 g, 0.1 mmol) in ethanol (1 mL) was added to **1** (0.2 mmol) in hot ethanol (25 mL). The resultant mixture was stirred at 60 °C for ∼1 h, and the resultant solution was left to stand at −20 °C for ∼12 h. The solid formed was collected by filtration, washed with ethanol, and dried in vacuum (purity >95%). Elemental Anal., Calcd %: C, 58.99; H, 3.18; N, 9.83. Found %: C, 58.74; H, 3.22; N, 9.67. ICP-MS, Calcd %: Cu, 11.15; S, 11.25. Found %: Cu, 11.18; S, 11.39.

(*E*)-2-((Benzo[*d*]thiazol-2-ylimino)methyl)-4-chlorophenol−$CuCl_2$ (5). $CuCl_2{\cdot}2H_2O$ (0.017 g, 0.1 mmol) in ethanol (1 mL) was added to **2** (0.2 mmol) in hot ethanol (25 mL). The resultant mixture was stirred at 60 °C for ∼1 h, and the resultant solution was left to stand at −20 °C for ∼12 h. The solid formed was collected by filtration, washed with ethanol, and dried in vacuum (purity >95%). Elemental Anal., Calcd %: C, 52.63; H, 2.52; N, 8.77. Found %: C, 52.94; H,2.54; N, 8.61. ICP-MS, Calcd %: Cu, 9.94; S, 10.04. Found %: Cu, 9.66; S, 10.08.

(*E*)-2-((Benzo[*d*]thiazol-2-ylimino)methyl)-4-nitrophenol−$CuCl_2$ (6). $CuCl_2{\cdot}2H_2O$ (0.017 g, 0.1 mmol) in ethanol (1 mL) was added to **3** (0.2 mmol) in hot ethanol (25 mL). The resultant mixture was stirred at 60 °C for ∼1 h, and the resultant solution was left to stand at −20 °C for ∼12 h. The solid formed was collected by filtration, washed with ethanol, and dried in vacuum (purity >95%). Elemental Anal., Calcd %: C, 50.94; H, 2.44; N, 12.73. Found %: C, 50.82; H, 2.34; N, 12.51. ICP-MS, Calcd %: Cu, 9.63; S, 9.71. Found %: Cu, 9.41; S, 9.87.

Cu^{2+} Binding Stoichiometry and Binding Affinity. Cu^{2+} binding stoichiometry and binding affinity were determined by UV−vis. Because the compounds are slightly soluble in water, 10 mM stock solutions were prepared in DMSO. In each titration, the solvent composition in the vessel was 50% (v/v) DMSO/buffer (10 mM HEPES, 150 mM NaCl, pH 6.6). For each compound, the binding constant was determined by titration of a 0.050 mM solution of the compound with microadditions of 1 mM $CuCl_2$ standard solution. Spectra were recorded after 5 min incubation at room temperature. Data were fitted to the theoretical equations by using the nonlinear least-squares fitting procedure implemented with the Origin 7.5 program.

Metal Ion Selectivity Studies. The interaction of compounds **1**−**3** with other metal ions was determined using UV−vis. To investigate the metal binding ability of compounds **1**−**3**, solutions of the ligands (50 or 100 μM in 50% (v/v) DMSO/buffer (10 mM HEPES, 150 mM NaCl, pH 6.6)) were prepared and treated with 0.5 equiv of $MgCl_2$, $CaCl_2$, $AlCl_3$, $FeCl_3$, $CoCl_2$, $NiCl_2$, or $ZnCl_2$. Spectra were recorded after 5 min incubation at room temperature. The metal ion selectivity of compounds **1**−**3** for Cu^{2+} over other metal ions was determined by UV−vis. To solutions of compounds **1**−**3** (50 or 100 μM in 50% (v/v) DMSO/buffer (10 mM HEPES, 150 mM NaCl, pH 6.6)), 25 or 50 μM of metal salt ($MgCl_2$, $CaCl_2$, $AlCl_3$, $FeCl_3$, $CoCl_2$, $NiCl_2$, or $ZnCl_2$) was added. The solution was incubated at room temperature for 5 min, the spectrum was recorded, and then 25 or 50 μM $CuCl_2$ was added. The resulting solution was mixed well, and the spectrum was recorded after additional 5 min incubation at room temperature. Selectivity was quantified by comparing and normalizing the absorbance values of the metal−ligand complex at λ = 460 nm to the absorbance of the solution at this wavelength after the addition of $CuCl_2$.

Aβ Sample Preparation. Aβ1−40 (lot no. U10012) was purchased from American Peptide and prepared as previously described.[38] Briefly, the powered Aβ peptide was first dissolved in 1,1,1,3,3,3-hexafluoro-2-propanol (HFIP) at the concentration of 1 mg/mL. The solution was shaken at 4 °C for 2 h in a sealed vial for further dissolution and was then stored at −20 °C as a stock solution. Before use, the solvent HFIP was removed by evaporation under a gentle stream of nitrogen and peptide was dissolved in water. Cu^{2+} induced aggregation of Aβ 1−40 was accomplished by mixing an aliquot of the peptides and $CuCl_2$ at a molar ratio of 1:1 into 10 mM HEPES (150 mM NaCl, pH 6.6) at 37 °C for 24 h. Aβ1−40 self-aggregation was accomplished by mixing an aliquot of the peptides from the stock solution into aggregation buffer (10 mM HEPES in 150 mM NaCl, pH 7.3) at 37 °C for 7 days. Due to the poor solubility of compounds **1**−**3** in water or media, the final amount of DMSO used in all biological experiment is 2% (v/v).

Light Scattering Measurements. Aβ aggregation were monitored in a Jasco-FP6500 spectrofluorometer by following the increase in light scattering using a 1.0 cm quartz cuvette lightening the samples at 320 nm and collecting scattered light at 90° angles at 320 nm. Light scattering by the buffer was used as baseline.

ThT Fluorescence Measurements. All of the measurements were recorded in a fluorescence spectrophotometer (JASCO FP-6500) at room temperature with excitation wavelength 444 nm. Fluorescence data at 480 nm were collected after 5 min to ensure that thermal equilibrium had been achieved. ThT was kept in excess at a final concentration of 10 μM.

Atomic Force Microscopy Study. For the atomic force microscopy (AFM) measurements, samples were diluted with deionized H_2O to yield a final concentration of 1 μM. Then the sample (20 μL) was applied onto freshly cleaved muscovite mica and allowed to dry. Data were acquired in the tapping mode on a Nanoscope V multimode atomic force microscope (Veeco Instruments, USA).

Light-Emission Measurements. Light emission was performed by using a photon-counting spectrometer (ultra-weak luminescence analyzer, BPCL-2-TGC) equipped with a cooled photomultiplier detection system, connected to a computer. Before the samples analyses, the background light was recorded and integrated. This background was subtracted from the recorded integrated spectra of the respective samples. Sample analyses were performed by adding the sample solution (10 μL) to luminol (10 μM) and HRP (3 U/mL) in buffer solution (150 μL; 150 mM Tris; pH 8.8) in a cuvette.

SOD Activity Determination. The SOD activity of the complexes was assayed by measuring inhibition of the photoreduction of nitro blue tetrazolium (NBT), by a method slightly modified from that originally described by Beauchamps and Fridovich. The solutions containing riboflavin (2×10^{-5} M), methionine (0.013 M), NBT (7.5×10^{-5} M), and complex of various concentrations were prepared with 50 mM phosphate buffer (pH 7.8). The mixtures were illuminated by a lamp with a constant light intensity for 10 min at 25 °C. After illumination, immediately the absorbance was measured at 560 nm. The entire reaction assembly was enclosed in a box lined with aluminum foil. Identical tubes with the reaction mixture were kept in the dark and served as blanks. Inhibition percentage was calculated according to the following formula: % inhibition = $[(A_0 - A)/A_0] \times 100$, where A_0 is the absorbance of the control and A is the absorbance of the samples. The IC_{50} value, which obtained from linear regression plots between percent SOD activities versus their concentrations, represents the concentration of the SOD mimic that induces a 50%

inhibition of the reduction of NBT. The SOD activities of test compounds were assayed in triplicate.

Intracellular Determination of ROS. The generation of reactive oxygen radicals was monitored using 2′,7′-dichlorofluorescein diacetate (DCFH-DA). This dye is a nonfluorescent compound which readily diffuses into the cells and reacts with intracellular free radicals. The product is dichlorofluorescein (DCF), which is a fluorophor. The DCF fluorescence intensity correlates with the amount of intracellular reactive oxygen radicals. To do the test, the DCFH-DA solution (20 μM) was added to the cells and the mixture was incubated at 37 °C for 1 h. The cells were then washed twice with PBS and, finally, the fluorescence intensity was monitored on a fluorescence spectrofluorometer (JASCO FP-6500) with excitation and emission wavelengths of 485 and 530 nm, respectively.

Cell Toxicity Assays. PC12 cells (rat pheochromocytoma, American Type Culture Collection) were cultured in IMDM (Gibco BRL) medium supplemented with 5% FBS, 10% horse serum in a 5% CO_2 humidified environment at 37 °C. For the MTT (3-(4,5-dimethylthiazol-2-yl)-2,5-diphenyltetrazolium bromide, Sigma-Aldrich) assay, cells were plated at a density of 10000 cells per well on 96-well plates, followed by introduction of Aβ (5 μM), $CuCl_2$ (5 μM), and a chelator (10 or 50 μM) 24 h later. After 48 h, the cells were treated with 10 μL MTT (5 mg/mL in PBS) for 4 h at 37 °C and then were lysed in DMSO for 10 min at room temperature in the dark. Absorbance values of formazan were determined at 570 nm with an automatic plate reader.

■ ASSOCIATED CONTENT

Ⓢ Supporting Information

UV−vis titration of compounds **2** and **3** with Cu^{2+}; metal ion selectivity studies; capture Cu^{2+} from Aβ by compounds **1**−**3** characterized by UV−vis spectrum; Cu^{2+} competitive binding experiment; the model structures of complexes **4**−**6**; fluorescence titration of Aβ with compounds **1**−**3** and metal complexes; effect of compounds **1**−**3** on Aβ self-assembly by ThT fluorescence assay; absorption spectra of complexes **4**−**6** in the presence (red line) of Aβ40; SOD activity of compounds **1**−**3** and SOD enzyme. Effect of compounds **1**−**3** on PC12 cell viability. This material is available free of charge via the Internet at http://pubs.acs.org.

■ AUTHOR INFORMATION

Corresponding Author

*Phone: (+86) 431-85262656. Fax: (+86) 431-85262656. E-mail: xqu@ciac.jl.cn.

Author Contributions

[§]J.G. and M.L. contributed equally to this work.

Notes

The authors declare no competing financial interest.

■ ACKNOWLEDGMENTS

Financial support by 973 Project (2011CB936004, 2012CB720602), NSFC (20831003, 90813001, 20833006, 90913007, 20903086), and Fund from CAS.

■ ABBREVIATIONS USED

AD, Alzheimer's disease; Aβ, amyloid β peptide; ROS, reactive oxygen species; BBB, blood−brain barrier; ThT, thioflavin T; CQ, clioquinol; SOD, superoxide dismutase

■ REFERENCES

(1) Blennow, K.; de Leon, M. J.; Zetterberg, H. Alzheimer's disease. *Lancet* **2006**, *368*, 387−403.

(2) (a) Hardy, J. Testing times for the "amyloid cascade hypothesis". *Neurobiol. Aging* **2002**, *23*, 1073−1074. (b) Hardy, J.; Selkoe, D. J. The amyloid hypothesis of Alzheimer's disease: progress and problems on the road to therapeutics. *Science* **2002**, *297*, 353−356.

(3) Bush, A. I. The metallobiology of Alzheimer's disease. *Trends Neurosci.* **2003**, *26*, 207−214.

(4) Lovell, M. A.; Robertson, J. D.; Teesdale, W. J.; Campbell, J. L.; Markesbery, W. R. Copper, iron and zinc in Alzheimer's disease senile plaques. *J. Neurol. Sci.* **1998**, *158*, 47−52.

(5) Stine, W. B., Jr.; Dahlgren, K. N.; Krafft, G. A.; LaDu, M. J. In vitro characterization of conditions for amyloid-beta peptide oligomerization and fibrillogenesis. *J. Biol. Chem.* **2003**, *278*, 11612−11622.

(6) (a) Sparks, D. L.; Schreurs, B. G. Trace amounts of copper in water induce beta-amyloid plaques and learning deficits in a rabbit model of Alzheimer's disease. *Proc. Natl. Acad. Sci. U.S.A.* **2003**, *100*, 11065−11069. (b) Syme, C. D.; Nadal, R. C.; Rigby, S. E.; Viles, J. H. Copper binding to the amyloid-beta (Abeta) peptide associated with Alzheimer's disease: folding, coordination geometry, pH dependence, stoichiometry, and affinity of Abeta-(1−28): insights from a range of complementary spectroscopic techniques. *J. Biol. Chem.* **2004**, *279*, 18169−18177. (c) Geng, J.; Yu, H. J.; Ren, J. S.; Qu, X. G. Rapid label-free detection of metal-induced Alzheimer's amyloid beta peptide aggregation by electrochemical method. *Electrochem. Commun.* **2008**, *10*, 1797−1800. (d) Yu, H.; Ren, J.; Qu, X. Different hydration changes accompanying copper and zinc binding to amyloid beta-peptide: water contribution to metal binding. *ChemBioChem* **2008**, *9*, 879−882.

(7) (a) Huang, X.; Atwood, C. S.; Hartshorn, M. A.; Multhaup, G.; Goldstein, L. E.; Scarpa, R. C.; Cuajungco, M. P.; Gray, D. N.; Lim, J.; Moir, R. D.; Tanzi, R. E.; Bush, A. I. The A beta peptide of Alzheimer's disease directly produces hydrogen peroxide through metal ion reduction. *Biochemistry* **1999**, *38*, 7609−7616. (b) Huang, X.; Cuajungco, M. P.; Atwood, C. S.; Hartshorn, M. A.; Tyndall, J. D.; Hanson, G. R.; Stokes, K. C.; Leopold, M.; Multhaup, G.; Goldstein, L. E.; Scarpa, R. C.; Saunders, A. J.; Lim, J.; Moir, R. D.; Glabe, C.; Bowden, E. F.; Masters, C. L.; Fairlie, D. P.; Tanzi, R. E.; Bush, A. I. Cu(II) potentiation of alzheimer abeta neurotoxicity. Correlation with cell-free hydrogen peroxide production and metal reduction. *J. Biol. Chem.* **1999**, *274*, 37111−37116.

(8) (a) Cherny, R. A.; Legg, J. T.; McLean, C. A.; Fairlie, D. P.; Huang, X.; Atwood, C. S.; Beyreuther, K.; Tanzi, R. E.; Masters, C. L.; Bush, A. I. Aqueous dissolution of Alzheimer's disease Abeta amyloid deposits by biometal depletion. *J. Biol. Chem.* **1999**, *274*, 23223−23228. (b) Cherny, R. A.; Atwood, C. S.; Xilinas, M. E.; Gray, D. N.; Jones, W. D.; McLean, C. A.; Barnham, K. J.; Volitakis, I.; Fraser, F. W.; Kim, Y.; Huang, X.; Goldstein, L. E.; Moir, R. D.; Lim, J. T.; Beyreuther, K.; Zheng, H.; Tanzi, R. E.; Masters, C. L.; Bush, A. I. Treatment with a copper−zinc chelator markedly and rapidly inhibits beta-amyloid accumulation in Alzheimer's disease transgenic mice. *Neuron* **2001**, *30*, 665−676.

(9) (a) Tjernberg, L. O.; Naslund, J.; Lindqvist, F.; Johansson, J.; Karlstrom, A. R.; Thyberg, J.; Terenius, L.; Nordstedt, C. Arrest of beta-amyloid fibril formation by a pentapeptide ligand. *J. Biol. Chem.* **1996**, *271*, 8545−8548. (b) Takahashi, T.; Mihara, H. Peptide and protein mimetics inhibiting amyloid beta-peptide aggregation. *Acc. Chem. Res.* **2008**, *41*, 1309−1318. (c) Frydman-Marom, A.; Rechter, M.; Shefler, I.; Bram, Y.; Shalev, D. E.; Gazit, E. Cognitive-performance recovery of Alzheimer's disease model mice by modulation of early soluble amyloidal assemblies. *Angew. Chem., Int. Ed. Engl.* **2009**, *48*, 1981−1986.

(10) (a) Yang, F.; Lim, G. P.; Begum, A. N.; Ubeda, O. J.; Simmons, M. R.; Ambegaokar, S. S.; Chen, P. P.; Kayed, R.; Glabe, C. G.; Frautschy, S. A.; Cole, G. M. Curcumin inhibits formation of amyloid beta oligomers and fibrils, binds plaques, and reduces amyloid in vivo. *J. Biol. Chem.* **2005**, *280*, 5892−5901. (b) Barnham, K. J.; Kenche, V. B.; Ciccotosto, G. D.; Smith, D. P.; Tew, D. J.; Liu, X.; Perez, K.; Cranston, G. A.; Johanssen, T. J.; Volitakis, I.; Bush, A. I.; Masters, C. L.; White, A. R.; Smith, J. P.; Cherny, R. A.; Cappai, R. Platinum-based inhibitors of amyloid-beta as therapeutic agents for Alzheimer's disease. *Proc. Natl. Acad. Sci. U.S.A.* **2008**, *105*, 6813−6818.

(c) Ehrnhoefer, D. E.; Bieschke, J.; Boeddrich, A.; Herbst, M.; Masino, L.; Lurz, R.; Engemann, S.; Pastore, A.; Wanker, E. E. EGCG redirects amyloidogenic polypeptides into unstructured, off-pathway oligomers. *Nature Struct. Mol. Biol.* **2008**, *15*, 558−566.
(11) Ouberai, M.; Dumy, P.; Chierici, S.; Garcia, J. Synthesis and Biological Evaluation of Clicked Curcumin and Clicked KLVFFA Conjugates as Inhibitors beta-Amyloid Fibril Formation. *Bioconjugate Chem.* **2009**, *20*, 2123−2132.
(12) Cairo, C. W.; Strzelec, A.; Murphy, R. M.; Kiessling, L. L. Affinity-based inhibition of beta-amyloid toxicity. *Biochemistry* **2002**, *41*, 8620−8629.
(13) (a) Zhang, G. B.; Leibowitz, M. J.; Sinko, P. J.; Stein, S. Multiple-peptide conjugates for binding beta-amyloid plaques of Alzheimer's disease. *Bioconjugate Chem.* **2003**, *14*, 86−92. (b) Chafekar, S. M.; Malda, H.; Merkx, M.; Meijer, E. W.; Viertl, D.; Lashuel, H. A.; Baas, F.; Scheper, W. Branched KLVFF tetramers strongly potentiate inhibition of beta-amyloid aggregation. *ChemBioChem* **2007**, *8*, 1857−1864. (c) Dolphin, G. T.; Chierici, S.; Ouberai, M.; Dumy, P.; Garcia, J. A multimeric quinacrine conjugate as a potential inhibitor of Alzheimer's beta-amyloid fibril formation. *ChemBioChem* **2008**, *9*, 952−963.
(14) (a) Ghadiri, M. R.; Soares, C.; Choi, C. Design of an Artificial 4-Helix Bundle Metalloprotein Via a Novel Ruthenium(II)-Assisted Self-Assembly Process. *J. Am. Chem. Soc.* **1992**, *114*, 4000−4002. (b) M. Lieberman, M.; Sasaki, T. Iron(II) organizes a synthetic peptide into three-helix bundles. *J. Am. Chem. Soc.* **1991**, *113*, 1470−1471.
(15) (a) Wu, C.; Pike, V. W.; Wang, Y. Amyloid imaging: from benchtop to bedside. *Curr. Top. Dev. Biol.* **2005**, *70*, 171−213. (b) Ono, M.; Hayashi, S.; Kimura, H.; Kawashima, H.; Nakayama, M.; Saji, H. Push−pull benzothiazole derivatives as probes for detecting beta-amyloid plaques in Alzheimer's brains. *Bioorgan. Med. Chem.* **2009**, *17*, 7002−7007.
(16) Pardridge, W. M. Alzheimer's disease drug development and the problem of the blood−brain barrier. *Alzheimer's Dementia* **2009**, *5*, 427−432.
(17) Clark, D. E.; Pickett, S. D. Computational methods for the prediction of 'drug-likeness. *Drug Discovery Today* **2000**, *5*, 49−58.
(18) Ferrada, E.; Arancibia, V.; Loeb, B.; Norambuena, E.; Olea-Azar, C.; Huidobro-Toro, J. P. Stoichiometry and conditional stability constants of Cu(II) or Zn(II) clioquinol complexes; implications for Alzheimer's and Huntington's disease therapy. *Neurotoxicology* **2007**, *28*, 445−449.
(19) Choi, J. S.; Braymer, J. J.; Nanga, R. P.; Ramamoorthy, A.; Lim, M. H. Design of small molecules that target metal-A{beta} species and regulate metal-induced A{beta} aggregation and neurotoxicity. *Proc. Natl. Acad. Sci. U.S.A.* **2010**, *107*, 21990−21995.
(20) (a) Cordeiro, Y.; Machado, F.; Juliano, L.; Juliano, M. A.; Brentani, R. R.; Foguel, D.; Silva, J. L. DNA converts cellular prion protein into the beta-sheet conformation and inhibits prion peptide aggregation. *J. Biol. Chem.* **2001**, *276*, 49400−49409. (b) Ferrao-Gonzales, A. D.; Robbs, B. K.; Moreau, V. H.; Ferreira, A.; Juliano, L.; Valente, A. P.; Almeida, F. C.; Silva, J. L.; Foguel, D. Controlling {beta}-amyloid oligomerization by the use of naphthalene sulfonates: trapping low molecular weight oligomeric species. *J. Biol. Chem.* **2005**, *280*, 34747−34754.
(21) (a) Stine, W. B., Jr.; Snyder, S. W.; Ladror, U. S.; Wade, W. S.; Miller, M. F.; Perun, T. J.; Holzman, T. F.; Krafft, G. A. The nanometer-scale structure of amyloid-beta visualized by atomic force microscopy. *J. Protein Chem.* **1996**, *15*, 193−203. (b) Arimon, M.; Diez-Perez, I.; Kogan, M. J.; Durany, N.; Giralt, E.; Sanz, F.; Fernandez-Busquets, X. Fine structure study of Abeta1−42 fibrillogenesis with atomic force microscopy. *FASEB J.* **2005**, *19*, 1344−1346.
(22) (a) Hindo, S. S.; Mancino, A. M.; Braymer, J. J.; Liu, Y.; Vivekanandan, S.; Ramamoorthy, A.; Lim, M. H. Small molecule modulators of copper-induced Abeta aggregation. *J. Am. Chem. Soc.* **2009**, *131*, 16663−16665. (b) Rodriguez-Rodriguez, C.; Sanchez de Groot, N.; Rimola, A.; Alvarez-Larena, A.; Lloveras, V.; Vidal-Gancedo, J.; Ventura, S.; Vendrell, J.; Sodupe, M.; Gonzalez-Duarte, P. Design, selection, and characterization of thioflavin-based intercalation compounds with metal chelating properties for application in Alzheimer's disease. *J. Am. Chem. Soc.* **2009**, *131*, 1436−1451.
(23) M. Mammen, M.; Choi, S. K.; Whitesides, G. M. Polyvalent Interactions in Biological Systems: Implications for Design and Use of Multivalent Ligands and Inhibitors. *Angew. Chem., Int. Ed. Engl.* **1998**, *37*, 2755−2794.
(24) (a) Baldini, L.; Casnati, A.; Sansone, F.; Ungaro, R. Calixarene-based multivalent ligands. *Chem. Soc. Rev.* **2007**, *36*, 254−266. (b) Bowman, M. C.; Ballard, T. E.; Ackerson, C. J.; Feldheim, D. L.; Margolis, D. M.; Melander, C. Inhibition of HIV fusion with multivalent gold nanoparticles. *J. Am. Chem. Soc.* **2008**, *130*, 6896−6897. (c) Rosenzweig, B. A.; Ross, N. T.; Tagore, D. M.; Jayawickramarajah, J.; Saraogi, I.; Hamilton, A. D. Multivalent protein binding and precipitation by self-assembling molecules on a DNA pentaplex scaffold. *J. Am. Chem. Soc.* **2009**, *131*, 5020−5021.
(25) (a) Yoshiike, Y.; Tanemura, K.; Murayama, O.; Akagi, T.; Murayama, M.; Sato, S.; Sun, X.; Tanaka, N.; Takashima, A. New insights on how metals disrupt amyloid beta-aggregation and their effects on amyloid-beta cytotoxicity. *J. Biol. Chem.* **2001**, *276*, 32293−32299. (b) Zou, J.; Kajita, K.; Sugimoto, N. Cu(2+) Inhibits the Aggregation of Amyloid beta-Peptide(1−42) in vitro. *Angew. Chem., Int. Ed. Engl.* **2001**, *40*, 2274−2277.
(26) Jun, S.; Saxena, S. The aggregated state of amyloid-beta peptide in vitro depends on Cu2+ ion concentration. *Angew. Chem., Int. Ed. Engl.* **2007**, *46*, 3959−3961.
(27) Tougu, V.; Karafin, A.; Zovo, K.; Chung, R. S.; Howells, C.; West, A. K.; Palumaa, P. Zn(II)- and Cu(II)-induced non-fibrillar aggregates of amyloid-beta (1−42) peptide are transformed to amyloid fibrils, both spontaneously and under the influence of metal chelators. *J. Neurochem.* **2009**, *110*, 1784−1795.
(28) Rauk, A. The chemistry of Alzheimer's disease. *Chem. Soc. Rev.* **2009**, *38*, 2698−2715.
(29) Miranda, S.; Opazo, C.; Larrondo, L. F.; Munoz, F. J.; Ruiz, F.; Leighton, F.; Inestrosa, N. C. The role of oxidative stress in the toxicity induced by amyloid beta-peptide in Alzheimer's disease. *Prog. Neurobiol.* **2000**, *62*, 633−648.
(30) Li, F.; Calingasan, N. Y.; Yu, F.; Mauck, W. M.; Toidze, M.; Almeida, C. G.; Takahashi, R. H.; Carlson, G. A.; Flint Beal, M.; Lin, M. T.; Gouras, G. K. Increased plaque burden in brains of APP mutant MnSOD heterozygous knockout mice. *J. Neurochem.* **2004**, *89*, 1308−1312.
(31) Melov, S.; Adlard, P. A.; Morten, K.; Johnson, F.; Golden, T. R.; Hinerfeld, D.; Schilling, B.; Mavros, C.; Masters, C. L.; Volitakis, I.; Li, Q. X.; Laughton, K.; Hubbard, A.; Cherny, R. A.; Gibson, B.; Bush, A. I. Mitochondrial oxidative stress causes hyperphosphorylation of tau. *PLoS One* **2007**, *2*, e536.
(32) Esposito, L.; Raber, J.; Kekonius, L.; Yan, F.; Yu, G. Q.; Bien-Ly, N.; Puolivali, J.; Scearce-Levie, K.; Masliah, E.; Mucke, L. Reduction in mitochondrial superoxide dismutase modulates Alzheimer's disease-like pathology and accelerates the onset of behavioral changes in human amyloid precursor protein transgenic mice. *J. Neurosci.* **2006**, *26*, 5167−5179.
(33) Massaad, C. A.; Washington, T. M.; Pautler, R. G.; Klann, E. Overexpression of SOD-2 reduces hippocampal superoxide and prevents memory deficits in a mouse model of Alzheimer's disease. *Proc. Natl. Acad. Sci. U.S.A.* **2009**, *106*, 13576−13581.
(34) Sompol, P.; Ittarat, W.; Tangpong, J.; Chen, Y.; Doubinskaia, I.; Batinic-Haberle, I.; Abdul, H. M.; Butterfield, D. A.; St. Clair, D. K. A neuronal model of Alzheimer's disease: an insight into the mechanisms of oxidative stress-mediated mitochondrial injury. *Neuroscience* **2008**, *153*, 120−130.
(35) Wu, Y.; Wang, D. A new class of natural glycopeptides with sugar moiety-dependent antioxidant activities derived from Ganoderma lucidum fruiting bodies. *J. Proteome Res.* **2009**, *8*, 436−442.
(36) (a) Guilloreau, L.; Combalbert, S.; Sournia-Saquet, A.; Mazarguil, H.; Faller, P. Redox chemistry of copper-amyloid-beta: the generation of hydroxyl radical in the presence of ascorbate is linked to redox-potentials and aggregation state. *ChemBioChem* **2007**, *8*, 1317−1325. (b) Jiang, D.; Men, L.; Wang, J.; Zhang, Y.; Chickenyen,

S.; Wang, Y.; Zhou, F. Redox reactions of copper complexes formed with different beta-amyloid peptides and their neuropathological relevance. *Biochemistry* **2007**, *46*, 9270−9282.
(37) Ji, H. F.; Zhang, H. Y. A new strategy to combat Alzheimer's disease. Combining radical-scavenging potential with metal-protein-attenuating ability in one molecule. *Bioorg. Med. Chem. Lett.* **2005**, *15*, 21−24.
(38) (a) Geng, J.; Zhao, C.; Ren, J.; Qu, X. Alzheimer's disease amyloid beta converting left-handed Z-DNA back to right-handed B-form. *Chem. Commun.* **2010**, *46*, 7187−7189. (b) Yu, H.; Ren, J.; Qu, X. Time-dependent DNA condensation induced by amyloid beta-peptide. *Biophys. J.* **2007**, *92*, 185−191. (c) Geng, J.; Li, M.; Ren, J.; Wang, E.; Qu, X. Polyoxometalates as inhibitors of the aggregation of amyloid beta peptides associated with Alzheimer's disease. *Angew. Chem., Int. Ed. Engl.* **2011**, *50*, 4184−4188.
(39) Goedert, M.; Spillantini, M. G. A century of Alzheimer's disease. *Science* **2006**, *314*, 777−781.
(40) Klafki, H. W.; Staufenbiel, M.; Kornhuber, J.; Wiltfang, J. Therapeutic approaches to Alzheimer's disease. *Brain* **2006**, *129*, 2840−2855.